

Point-contact spectroscopic studies on normal and superconducting AFe_2As_2 -type iron-pnictide single crystals

Xin Lu¹, W. K. Park¹, H. Q. Yuan², G. F. Chen³, G. L. Luo³, N. L. Wang³, A. S. Sefat⁴, M. A. McGuire⁴, R. Jin⁴, B. C. Sales⁴, D. Mandrus⁴, J. Gillett⁵, Suchitra E. Sebastian⁵ and L. H. Greene¹

¹ Department of Physics and Fredrick Seitz Materials Research Lab., University of Illinois at Urbana-Champaign, IL 61801

² Department of Physics, Zhejiang University, Hangzhou 310027, China

³ Institute of Physics, Chinese Academy of Science, Beijing 100190, China

⁴ Materials Science & Technology Division, Oak Ridge National Lab., Oak Ridge, TN 37831

⁵ Cavendish Laboratory, Cambridge University, JJ Thomson Avenue, Cambridge CB30HE, U.K.

E-mail: xinlu@illinois.edu

Abstract. Point-contact Andreev reflection spectroscopy (PCARS) is applied to investigate the gap structure in iron pnictide single crystal superconductors of the AFe_2As_2 ($\text{A}=\text{Ba}, \text{Sr}$) family (“Fe-122”). The observed point-contact junction conductance curves, $G(V)$, can be divided into two categories: one where Andreev reflection is present for both $(\text{Ba}_{0.6}\text{K}_{0.4})\text{Fe}_2\text{As}_2$ and $\text{Ba}(\text{Fe}_{0.9}\text{Co}_{0.1})_2\text{As}_2$, and the other with a $V^{2/3}$ background conductance universally observed extending even up to 100 meV for $\text{Sr}_{0.6}\text{Na}_{0.4}\text{Fe}_2\text{As}_2$ and $\text{Sr}(\text{Fe}_{0.9}\text{Co}_{0.1})_2\text{As}_2$. The latter is also observed in point-contact junctions on the nonsuperconducting parent compound BaFe_2As_2 . Mesoscopic phase-separated coexistence of magnetic and superconducting orders is considered to explain distinct behaviors in the superconducting samples. For $\text{Ba}_{0.6}\text{K}_{0.4}\text{Fe}_2\text{As}_2$, double peaks due to Andreev reflection with strongly-sloping background are frequently observed for point-contacts on freshly-cleaved c-axis surfaces. If normalized by a background baseline and analyzed by the Blonder-Tinkham-Klapwijk model, the data show a gap size $\sim 3.0\text{-}4.0$ meV with $2\Delta_0/k_B T_c \sim 2.0\text{-}2.6$, consistent with the smaller gap size reported in the LnFeAsO family (“Fe-1111”). For the $\text{Ba}(\text{Fe}_{0.9}\text{Co}_{0.1})_2\text{As}_2$, $G(V)$ curves typically display a zero-bias conductance peak.

1. Introduction

The recently-discovered iron-based superconductors [1] have emerged as a whole new family of high temperature superconductors, which are complimentary to the study of cuprates. They have attracted intensive study in the community focusing on their physical properties and potential applications. Reminiscent of cuprates, the antiferromagnetic (AFM) phase in the parent compounds is suppressed with chemical doping or higher pressure, and it is proposed that superconductivity in iron pnictides may originate from AFM fluctuations [2]. It is pointed out that there are also vital differences in that the AFM ground state in the cuprates and Fe-pnictides are Mott-insulator and metallic, respectively. Soon after the discovery of Fe-pnictides, ARPES and quantum oscillation measurements have revealed disconnected hole-like bands around the $\Gamma(0,0)$ point and electron-like bands around the $M(\pi,\pi)$ point on the FS [3, 4, 5, 6, 7]. The order parameter (OP) symmetry in the cuprates has been determined to be $d_{x^2-y^2}$, while it is still not known for the iron-pnictides. A first step in unveiling the mechanism of the new family of superconductors is to determine the pairing symmetry. An extended s-wave gap structure with a sign reversal ($s\pm$) on different FSs is proposed by I. Mazin [2] where the hole-like and electron-like bands are fully-gapped and have a π phase shift in the superconducting state. A fully-gapped state has been confirmed by different experimental techniques such as ARPES [3, 4, 5, 6], penetration depth [8], μ SR [9, 10], H_{c1} [11] and specific heat measurements [12]. However, a universal power law rather than exponential behavior is observed in the London penetration depth measurement for $RFeAsO_{0.9}F_{0.1}$ ($R=Nd, La$) [13], and $Ba(Fe_{1-x}Co_x)_2As_2$ at various doping levels [14, 15]. The Hebel-Slichter coherent peak is absent in NMR measurements [16, 17] and it is argued that is a natural consequence of the extended $s\pm$ model in the superconducting state [18].

Point-contact Andreev reflection spectroscopy (PCARS) is a powerful tool to investigate the gap structure and OP symmetry in superconductors. A good example is the case of MgB_2 , where two gaps, originating from σ and π bands, are clearly present in the point-contact spectra, and also through directional PCARS measurements, the gap dependences on temperature and magnetic field are systematically revealed [20, 21, 22]. Park *et al.* successfully applied PCARS to reveal the $d_{x^2-y^2}$ symmetry of the superconducting OP in $CeCoIn_5$ [23]. Shortly after the discovery of the superconducting $LnFeAsO$ (Fe-1111) family, some PCARS measurements have been carried out, but the results are not yet conclusive, partly due to the polycrystalline nature of the samples. Chen *et al.* report a conventional BCS-like superconducting gap with $2\Delta_0/k_B T_c \sim 3.7$ for $SmFeAsO_{0.85}F_{0.15}$ [24], while multiple gaps are claimed by other groups with different detailed structures in the initial stage [25, 26, 27, 28, 29]. Among those who claim multiple gaps, some merging agreements are being reached where $2\Delta_1/k_B T_c \sim 2-3$ and $2\Delta_2/k_B T_c \sim 7-9$. In this paper, we apply PCARS to different AFe_2As_2 -type superconducting single crystals to elucidate their gap structure and OP symmetry.

2. Experiment

AFe₂As₂-type (Fe-122) parent compound and various superconducting single crystals are grown out of FeAs flux by a high temperature solution method, such as parent compound BaFe₂As₂ ($T_N \sim 135$ K), electron-doped superconducting A(Fe_{0.9}Co_{0.1})₂As₂ (A=Ba or Sr, $T_c \sim 22$ K) [30], and hole-doped superconducting (Ba_{0.6}K_{0.4})Fe₂As₂ ($T_c \sim 37$ K) and (Sr_{0.6}Na_{0.4})Fe₂As₂ ($T_c \sim 35$ K)[31]. The crystals have natural c-axis facets and are cleaved in the air to expose fresh and shiny surfaces before mounting on the sample holder. A sharp Au tip prepared by electrochemical etch [32] is engaged onto the sample surface with a conventional differential micrometer mechanism [33]. The contact between the Au normal metal and Fe-122 crystals is made after cooling to ~ 2 K. The junction conductance $dI/dV = G$, as a function of the bias voltage V , is recorded by the standard ac lock-in technique, where the superconductor is always biased positively. Contacts may be lost due to vibration or instability in thermal contraction. Here we report data obtained after dozens of contacts have been made on each crystal, and some with changing temperature up to the bulk T_c and magnetic field up to 9 Tesla.

3. Results and Discussions

Two different categories of $G(V)$ curves are observed for point-contacts on these Fe-122 superconducting crystals: (1) For (Ba,K)Fe₂As₂ and Ba(Fe,Co)₂As₂, Andreev reflection signals are observed but distinct from each other; and (2) For (Sr,Na)Fe₂As₂ and Sr(Fe,Co)₂As₂, in the absence of Andreev reflection, a universal power law behavior is seen. The latter is also observed for the point-contact on the non-superconducting parent compound BaFe₂As₂. Results and discussions are presented here for each case separately.

3.1. (Ba,K)Fe₂As₂

For the (Ba,K)Fe₂As₂ crystals, representatives of the most frequently observed $G(V)$ curves at low temperatures (~ 2 K) are shown in Figure 1. The prominent features are the two peaks at $\sim \pm 3$ meV and a strongly sloping background. A hump structure can also be noticed around ± 15 meV as indicated by arrows, and a small conductance asymmetry is systematically observed. Similar broad backgrounds and asymmetries are reported in the recent point-contact measurement on SmFeAsO_{0.8}F_{0.2}, where the sloping background is claimed to disappear around the Neel temperature (~ 140 K) of the parent compound [29]. The temperature dependence as shown in Figure 2(a) verifies that the low-bias conductance enhancement is due to Andreev reflection. Although the junction resistance changes with temperature, the Andreev reflection signal disappears only above the bulk T_c , giving confidence that we probe the bulk gap. The sloping background survives above T_c so it does not originate from superconductivity and must be due to some other scattering mechanism.

Since the (Ba,K)Fe₂As₂ material is known to be reactive in air, we try to minimize exposure time between cleavage and cooldown. The usual time is about 30 minutes. We investigate the effect of a 1 week air exposure as shown in Figure 2(b). The Andreev reflection signal is lost below 16.6 K, lower than that of the bulk. This indicates the air exposure degrades the surface and suppresses the superconductivity and that cleavage minimizes the surface degradation. We note the sloping background does not change with the air exposure.

For the gap analysis, we normalize the conductance for the cleaved surfaces to the extrapolated baseline as shown in Figure 3(a). The normalized data are then analyzed by the single-gap Blonder-Tinkham-Klapwijk (BTK) model [34, 35]. The best fit for the energy gap is $\sim 3.0 - 4.0$ meV, so $2\Delta_0/k_B T_c \sim 2.0 - 2.6$, smaller than the BCS weak coupling ratio of 3.52. This value is comparable with the smaller gap size probed by PCARS on polycrystalline samples of LaFeAsO_{1-x}F_x [26], NdFeAsO_{0.9}F_{0.1} [27], and SmFeAsO_{0.8}F_{0.2} [29]. We stress that our materials are “Fe-122” single crystals, and we probe in the c-axis orientation. This may account for us not observing the larger gap as follows: An ARPES study on (Ba,K)Fe₂As₂ reveals an isotropic but FS sheet-dependent gap structure, where the β band has an averaged gap size $\sim 5.8 \pm 0.8$ meV with $2\Delta/k_B T_c \sim 3.6 \pm 0.5$ and the α, γ and δ bands have comparable gap sizes around 11-13 meV with $2\Delta/k_B T_c \sim 7.0 - 8.0$ [4]. Considering the FSs from band structure calculations, the α, γ and δ bands are highly 2-dimensional with cylindrical shapes while the β band is strongly 3-dimensional due to the $d_{3z^2-r^2}$ component [36]. The small gap observed here may correspond to the 3D β band. Because the Fermi velocity on the α, γ , and δ bands is mostly in the ab plane and perpendicular to the c-axis, these bands contribute a relatively small spectral weight for current flowing in the c-axis, and the coherent peaks from these larger-gap bands are almost absent in PCARS, similar to the case of MgB₂ [20]. Both gaps should then be observable if junction current is flowing within the ab plane. Szabó *et al.* report two superconducting gaps for PCARS measurement in the ab plane with $2\Delta_1/k_B T_c = 2.5 - 4$ and $2\Delta_2/k_B T_c = 9 - 10$ [37]. However, Andreev reflection is totally absent for their point-contact junctions in c-axis. This is distinct from our results and may be due to the sample difference.

The elastic and inelastic electron mean free paths, l_{el} and l_{in} , respectively, are not known for (Ba,K)Fe₂As₂ single crystals. However, it is generally believed that they are bad metals and l_{el} could be a few tens of nanometers, making it difficult to form a contact in the Sharvin ballistic limit, (contact diameter $d < l_{el}$). For the contact in the diffusive regime ($l_{el} < d < \sqrt{l_{el} l_{in}}$), dips may arise from the extra finite resistance of the superconducting electrode when the junction current at a finite voltage bias exceeds the critical current [38]. The humps in Figure 1 are a possible signature of shallow dips, possibly dimmed by the sloping background. As the point-contact is moved further away from the ballistic regime, the dip structure becomes more pronounced and a zero-bias conductance peak (ZBCP) is observed, rather than the usual double-peak. This is likely the case as shown in Figure 4(a) & (b) where a ZBCP is observed and the dips at ± 10 meV are more pronounced than in Figure 1. Although a peak at zero bias may

arise from Andreev bound states in a d-wave superconductor [39], the width, the lack of field dependence as shown in Figure 4 (c), and the pronounced dip structures together indicate the ZBCP is due to the contact not being in the Sharvin limit.

3.2. $Ba(Fe,Co)_2As_2$

Conductance curves for the point-contact junctions on cleaved $Ba(Fe,Co)_2As_2$ single crystals are shown as a function of contact resistance and temperature in Figures 5(a) and 5(b), respectively. For most contacts, a conductance enhancement at zero-bias with broad shoulders is observed. Note that with increasing temperature, the ZBCP disappears at the bulk T_c indicating it originates from Andreev reflection. A V-shape $G(V)$ is obtained when the tip is in gentle contact with the crystal hundreds of ohms junction resistance, and with increased tip pressure reducing the junction resistance, the conductance curve changes to the general ZBCP feature.

3.3. $BaFe_2As_2$, $(Sr,Na)Fe_2As_2$ & $Sr(Fe,Co)_2As_2$

Figure 6 (a) and (b) show the typical $G(V)$ curves with reduced conductance at lower voltage bias observed for the point-contact junctions on cleaved $(Sr,Na)Fe_2As_2$ and $Sr(Fe,Co)_2As_2$ surfaces. Similar features are also reported by other groups [27, 28]. We find the conductance shape does not change up to applied magnetic fields of 9 Tesla. There is no splitting of the zero-bias anomaly (ZBA) in the magnetic field, which may rule out the Kondo scattering as an origin. This ZBA feature, without Andreev reflection, is probably due to the absence of superconductivity in probed areas, even though the samples are checked to be superconducting. Conductance curves with this ZBA, as shown in Figure 6(c), are sometimes observed in the point-contact junctions on cleaved $(Ba,K)Fe_2As_2$ crystals. We have also observed the same ZBA feature for the nonsuperconducting parent compound $BaFe_2As_2$ single crystals even up to 200 meV, as shown in Figure 6(d), where SDW magnetic order exists. All the curves can be fit to a power law function $G(V) = G(0) + c * |V|^n$ with a power coefficient, $n \sim 2/3$. This may indicate a universal origin of this ZBA observed commonly among different crystals.

In the $BaFe_2As_2$ parent compound, a structure transition occurs at the antiferromagnetic ordering temperature, $T_N \sim 135$ K. A phase-separated coexistence of magnetic order and superconductivity in Fe-122 family is reported in recent muon spin rotation (μ SR) studies [40, 41, 43] with a magnetic correlation length > 100 Å. Park *et al.* demonstrate the mesoscopic phase-separated coexistence of magnetically ordered and non-magnetic states on a lateral scale of ~ 65 nm in the slightly underdoped $(Ba,K)Fe_2As_2$ system [40]. Whether such coexistence is an intrinsic electronic property for Fe-122 system or due to some crystalline inhomogeneity remains uncertain.

In investigating the possibility that the ZBA originates from magnetic order, we note magnetic order can be detected by PCARS [42]. A point-contact junction made on a superconducting region would exhibit Andreev reflection and one on a nonsuperconducting, magnetically ordered region would not. Instead, a signature due

to electron scattering from magnetic order may be detected. This may be the case for $(\text{Sr,Na})\text{Fe}_2\text{As}_2$ and $\text{Sr}(\text{Fe,Co})_2\text{As}_2$ where no Andreev reflection peak in $G(V)$ has been observed, and $G(V)$ curves with the ZBA are mostly observed. Goko et al. apply μSR to investigate $(\text{Ba,K})\text{Fe}_2\text{As}_2$ and $(\text{Sr,Na})\text{Fe}_2\text{As}_2$ single crystals (same source as ours) and argue that static magnetism sets in at temperatures well above the superconducting T_c . They estimate the superconducting volume fraction to be 50 % in $(\text{Ba,K})\text{Fe}_2\text{As}_2$ crystals and $\sim 90\%$ in $(\text{Sr,Na})\text{Fe}_2\text{As}_2$ crystals at low temperatures [43]. This is consistent with our more frequent observation of ZBA features in $(\text{Sr,Na})\text{Fe}_2\text{As}_2$ than $(\text{Ba,K})\text{Fe}_2\text{As}_2$ crystals.

Temperature dependent PCARS for the parent compound BaFe_2As_2 reveals the ZBA feature is broadened and reduced with increasing temperature. As the Neel temperature ($T_N \sim 135$ K) is crossed, no dramatic change in the spectra is observed but thermal population effects may mask changes in conductance due to the magnetic transition.

4. Summary

In conclusion, our PCARS measurement on the cleaved $(\text{Ba,K})\text{Fe}_2\text{As}_2$ single crystal surfaces shows a superconducting gap energy of ~ 4 meV when $G(V)$ curves are analyzed by the single-gap BTK model. For point-contacts on $\text{Ba}(\text{Fe,Co})_2\text{As}_2$, zero-bias peak is frequently observed due to Andreev reflection. A universal power law behavior of the $G(V)$ observed for PCARS on different Fe-122 superconducting samples may be a natural result of the mesoscopic phase-separated coexistence of magnetic and superconducting phases in the 122 system. More careful investigation is needed to understand the origin of the power-law ZBA behavior. Point-contact measurement in the ab-plane would be helpful to explore more detailed gap structure of these new unconventional superconductors.

Acknowledgments

We thank R. Hasch for technical support. This work at UIUC is supported by the U.S. DoE Award No. DEFG02-07ER46453 through the Frederick Seitz Materials Research Laboratory and the Center for Micro-analysis of Materials at UIUC. Xin Lu thanks the support by NSF DMR 07-06013. HQY is support by the National Science Foundation of China (Grant No.10874146,10934005), the National Basic Research Program of China (Grant No.2009CB929104) and Zhejiang Natural Science Foundation (ZJNSF R0690113). The work at ORNL is supported by Division of Materials Sciences and Engineering, Office of Basic Energy Sciences, DOE.

References

- [1] Kamihara Y, Watanabe T, Hirano M and Hosono H 2008 *J. Am. Chem. Soc.* **130** 3296
- [2] Mazin I I, Singh D J, Johannes M D and Du M H 2008 *Phys. Rev. Lett.* **101** 057003
- [3] Ding H *et al* 2008 *Europhys. Lett.* **83** 47001
- [4] Nakayama K *et al* 2009 *Europhys. Lett.* **85** 67002
- [5] Kondo T *et al* 2008 *Phys. Rev. Lett.* **101** 147003
- [6] Zhao L *et al* 2008 *Chin. Phys. Lett.* **25** 4402
- [7] Sebastian S E, Gillett J, Harrison N, Lau P H C, Mielke C H and Lonzarich G G 2008 *J. Phys.: Condens. Matter* **20** 422203
- [8] Hashimoto K *et al* 2009 *Phys. Rev. Lett.* **102** 017002
- [9] Aczel A A *et al* 2008 *Phys. Rev. B* **78** 214503
- [10] Drew A J *et al* 2008 *Phys. Rev. Lett.* **101** 097010
- [11] Ren C, Wang Z S, Luo H Q, Yang H, Shan L and Wen H-H 2008 *Phys. Rev. Lett.* **101** 257006
- [12] Mu G, Luo H Q, Wang Z S, Shan L, Ren C and Wen H-H 2009 *Phys. Rev. B* **79** 174501
- [13] Martin C *et al* 2009 *Phys. Rev. Lett.* **102** 247002
- [14] Gordon R T *et al* 2009 *Phys. Rev. Lett.* **102** 127004
- [15] Gordon R T, Martin C, Kim H, Ni N, Tanata M A, Schmalian J, Mazin I I, Bud'ko S L, Canfield P C and Prozorov R 2009 *Phys. Rev. B* **79** 100506(R)
- [16] Grafe H-J *et al* 2008 *Phys. Rev. Lett.* **101** 047003
- [17] Matano K, Ren Z A, Dong X L, Sun L L, Zhao Z X and Zheng G-q 2008 *Europhys. Lett.* **83** 57001
- [18] Parker D, Dolgov O V, Korshunov M M, Golubov A A and Mazin I I 2008 *Phys. Rev. B* **78** 134524
- [19] Luetkens H *et al* 2008 *Phys. Rev. Lett.* **101** 097009
- [20] Gonnelli R S, Daghero D, Ummarino G A, Stepanov V A, Jun J, Kazakov S M and Karpinski J 2002 *Phys. Rev. Lett.* **89** 247004
- [21] Gonnelli R S, Daghero D, Calzolari A, Ummarino G A, Dellarocca V and Stepanov V A 2004 *Phys. Rev. B* **69** 100504(R)
- [22] Yanson I K and Naidyuk Yu G 2004 *Low Temp. Phys.* **30** 261;
- [23] Park W K, Sarrao J L, Thompson J D and Greene L H 2008 *Phys. Rev. Lett.* **100** 177001
- [24] Chen T Y, Tesanovic Z, Liu R H, Chen X H and Chien C L 2008 *Nature* **453** 1224
- [25] Wang Y L, Shan L, Cheng P, Ren C and Wen H H 2009 *Supercond. Sci. Technol.* **22** 015018
- [26] Gonnelli R S, Daghero D, Tortello M, Ummarino G A, Stepanov V A, Kim J S and Kremer R S 2009 *Phys. Rev. B* **79** 184526
- [27] Samuely P, Szabó P, Pribulová Z, Tillman M E, Bud'ko S and Canfield P C 2009 *Supercond. Sci. Technol.* **22** 014003
- [28] Yates K A, Cohen L F, Ren Z-A, Yang J, Lu W, Dong X L and Zhao Z-X 2008 *Supercond. Sci. Technol.* **21** 092003
- [29] Daghero D, Tortello M, Gonnelli R S, Stepanov V A, Zhigadlo N D and Karpinski J 2008 arXiv: 0812.1141
- [30] Sefat A S, Jin R, McGuire M A, Sales B C, Singh D and Mandrus D 2008 *Phys. Rev. Lett.* **101** 117004
- [31] Chen G L, Li Z, Dong J, Li G, Hu W Z, Zhang X D, Song X H, Zheng P, Wang N L and Luo J L 2008 *Phys. Rev. B* **78** 224512
- [32] Park W K and Greene L H 2006 *Rev. Sci. Instru.* **77** 023905
- [33] Xin Lu, University of Illinois at Urbana Champaign, PhD thesis in preparation
- [34] Blonder G E, Tinkham M and Klapwijk T M 1982 *Phys. Rev. B* **25** 4515
- [35] Pleceník A, Grajcar M, Beňačka I C V, Seidel P and Pfuch A, 1994 *Phys. Rev. B* **49** 10016
- [36] Wang G T, Qian Y, Xu G, Dai X and Fang Z 2009 arXiv:0903.1385
- [37] Szabó P, Pribulová Z, Pristáš G, Bud'ko S L, Canfield P C and Samuely P 2009 *Phys. Rev. B* **79** 012503
- [38] Sheet G, Mukhopadhyay S and Raychaudhuri P 2004 *Phys. Rev. B* **69** 134507

- [39] Aprili M, Badica E and Greene L H 1999 *Phys. Rev. Lett.* **83** 4630
- [40] Park J T *et al* 2009 *Phys. Rev. Lett.* **102** 117006
- [41] Amato A, Khasanov R, Luetkens H and Klauss H H 2009 arXiv: 0901.3139
- [42] Park W K, Sarrao J L, Thompson J D, Pham L D, Fisk Z and Greene L H 2008 *Phys. B* **403** 731
- [43] Goko T *et al* 2009 *Phys. Rev. B* **80**, 024508

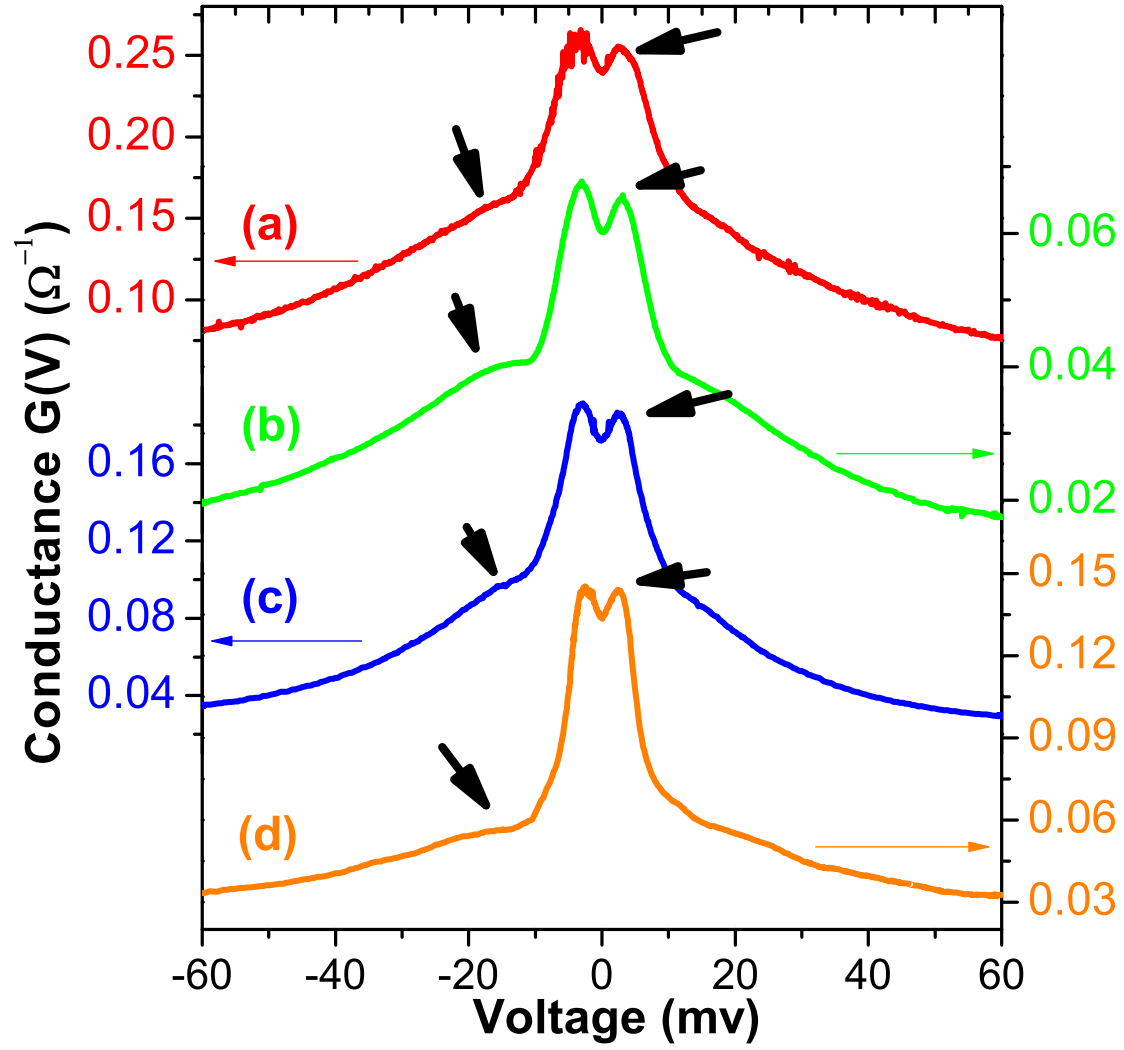


Figure 1. Differential conductance spectra $G(V)$ for the Au/(Ba_{0.6}K_{0.4})Fe₂As₂ point-contact junctions at low temperatures $T \sim 2$ K. The peak and hump structures are indicated by arrows nearby.

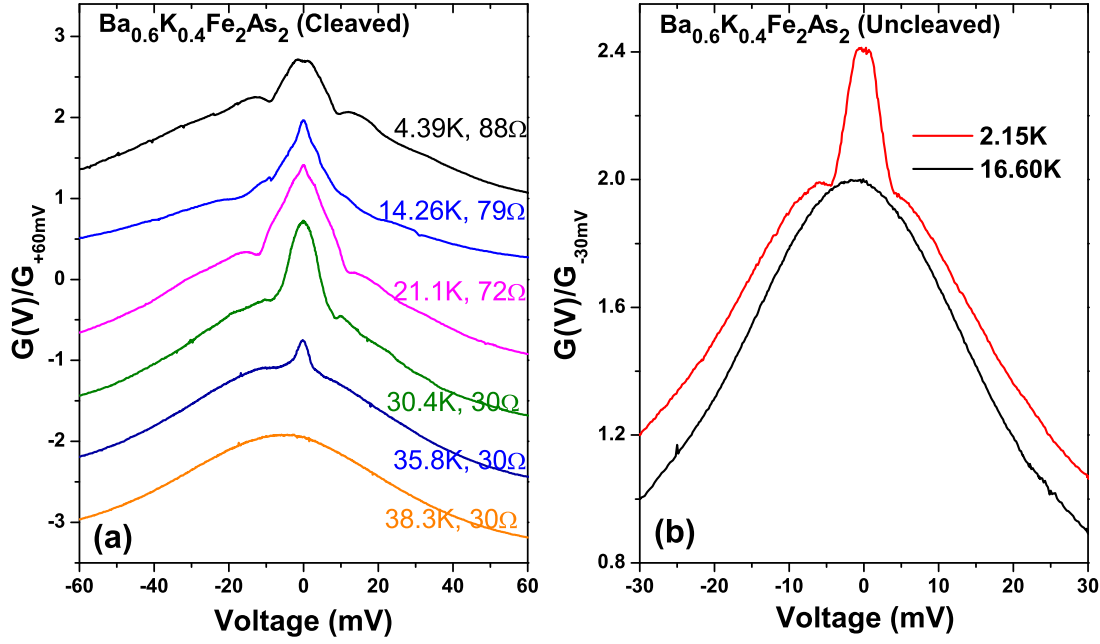


Figure 2. Temperature dependence of the conductance curves $G(V)$ for the $\text{Au}/(\text{Ba},\text{K})\text{Fe}_2\text{As}_2$ point-contact junctions on a (a) fresh-cleaved surface (the junction resistance changes with temperature due to instability of the contact) and (b) uncleaved surface. The curves are vertically shifted for clarity.

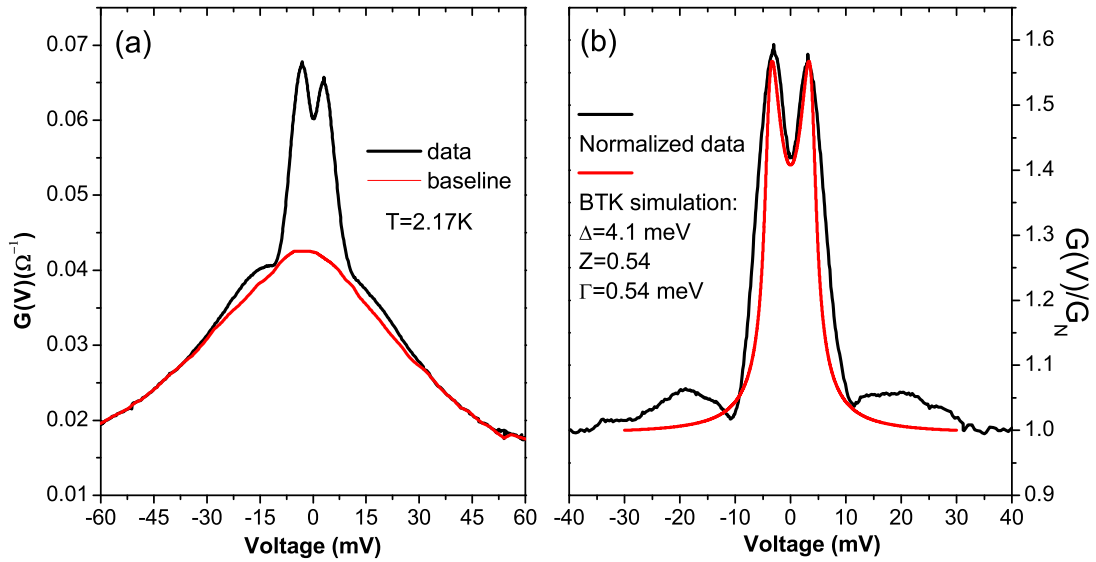


Figure 3. (a) Differential conductance curve $G(V)$ of a $\text{Au}/(\text{Ba},\text{K})\text{Fe}_2\text{As}_2$ point-contact junction and extrapolated background baseline; (b) The normalized conductance data and best fitting curve by BTK model.

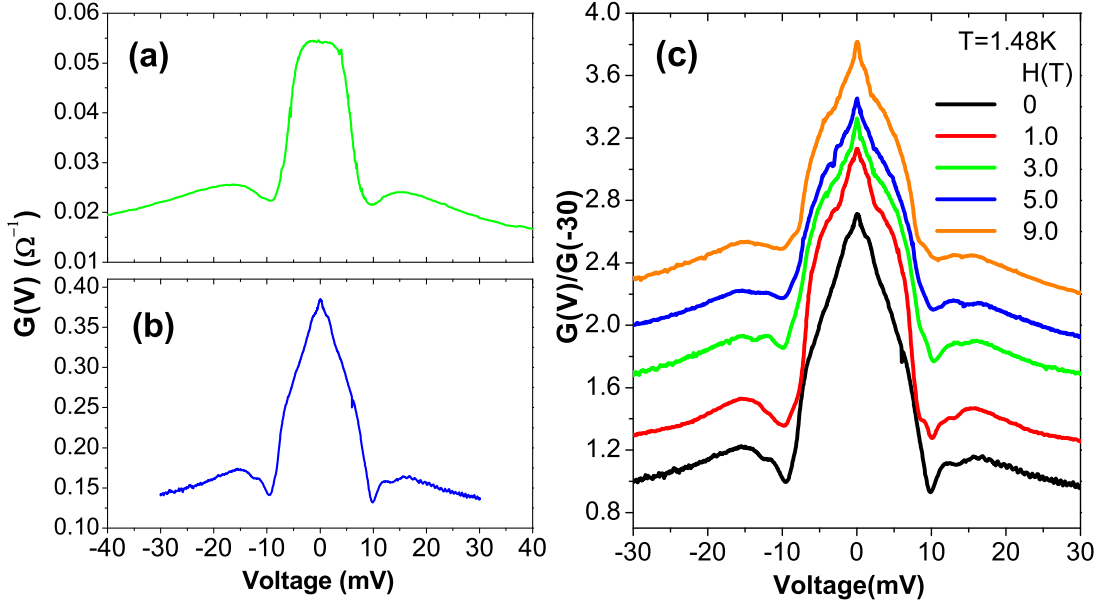


Figure 4. (a) & (b) Differential conductance curves $G(V)$ without double-peak structure for the Au/(Ba,K)Fe₂As₂ point-contact junctions. (c) the field dependence of the $G(V)$ in (b) at $T=1.48$ K. The curves are vertically shifted for clarity.

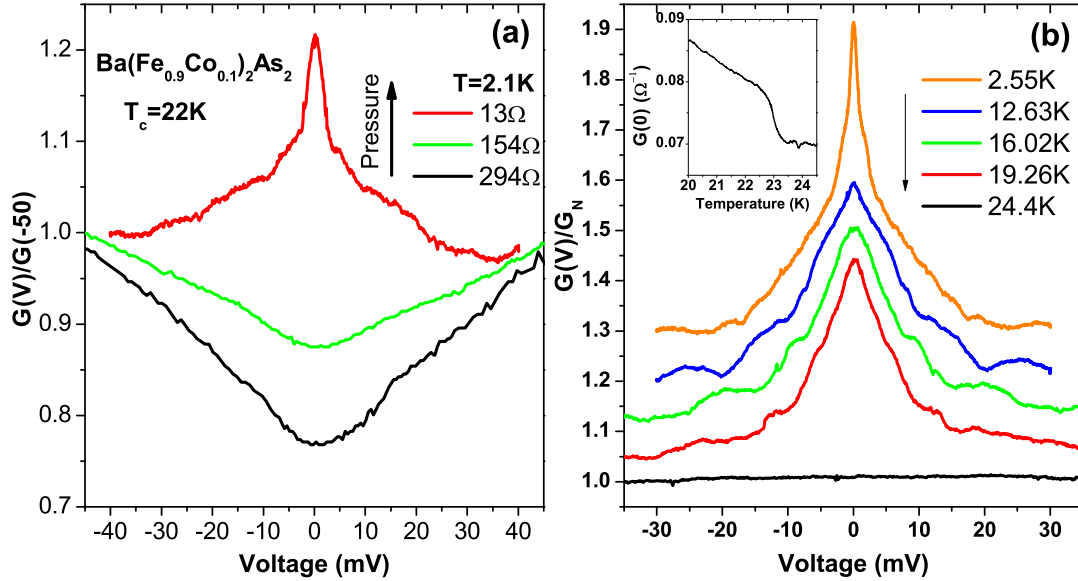


Figure 5. (a) The point-contact conductance curve, $G(V)$, evolving from V-shape to ZBCP with the increase of tip pressure at $T=2.1$ K; (b) The temperature dependence of $G(V)$ with ZBCP. The curves are vertically shifted for clarity. Inset shows the temperature evolution of the zero-bias conductance around the bulk T_c .

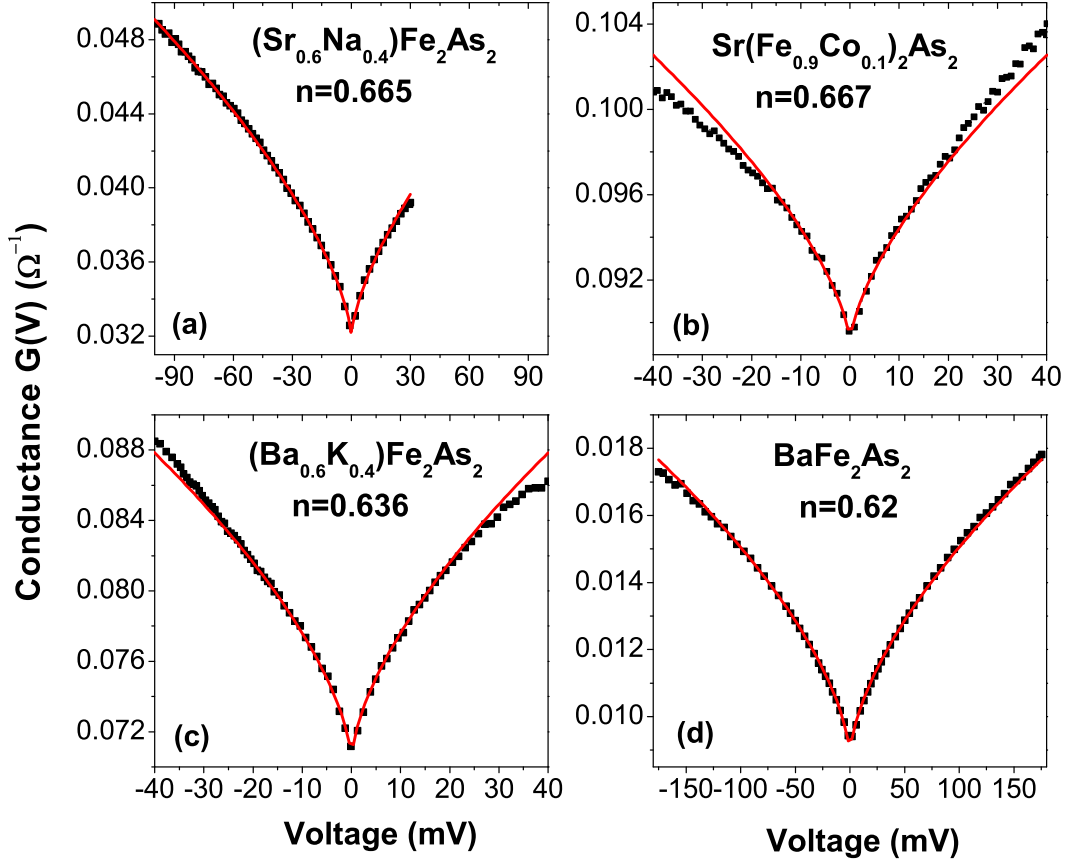


Figure 6. ZBA: $G(V)$ curves observed (black) and power law fit (red) with n as the fitted power coefficient for the point-contact junctions on (a) $(\text{Sr}_{0.6}\text{Na}_{0.4})\text{Fe}_2\text{As}_2$; (b) $\text{Sr}(\text{Fe}_{0.9}\text{Co}_{0.1})_2\text{As}_2$; (c) $(\text{Ba}_{0.6}\text{K}_{0.4})\text{Fe}_2\text{As}_2$; (d) BaFe_2As_2 .